

Colliding shock waves and hydrodynamics in small systems

Paul M. Chesler

Department of Physics, Harvard University, Cambridge, MA 02138, USA*

(Dated: February 19, 2022)

Using numerical holography, we study the collision of a planar sheet of energy with a bounded localized distribution of energy. The collision, which mimics proton-nucleus collisions, produces a localized lump of debris with transverse size $R \sim 1/T_{\text{eff}}$ with T_{eff} the effective temperature, and has large gradients and large transverse flow. Nevertheless, the postcollision evolution is well described by viscous hydrodynamics. Our results bolster the notion that debris produced in proton-nucleus collisions may be modeled using hydrodynamics.

Introduction.—Data on recent light-heavy ion collisions, including proton-nucleus collisions, indicate the presence of collective flow [1–4]. While alternative mechanisms for the origin of the flow have been proposed [5], the data are consistent with hydrodynamic evolution [6–8]. However, at experimentally accessible energies microscopic scales are likely not too different than the system size. This raises several questions. Is it theoretically consistent to apply hydrodynamics to systems whose size is of order microscopic scales? Is it consistent to neglect nonhydrodynamic degrees of freedom when gradients are large? What is the size of the smallest drop of liquid?

Since microscopic length and time scales typically decrease in the limit of strong coupling, it is natural to expect the domain of utility of hydrodynamics to be maximized at strong coupling. However, strongly coupled dynamics in QCD are notoriously difficult to study. Holographic duality [9] maps the dynamics of certain strongly coupled non-Abelian gauge theories onto the dynamics of classical gravity in one higher dimension. The process of quark-gluon plasma formation is mapped onto gravitational collapse and black hole formation with the ring down of the black hole encoding the relaxation of the plasma to a hydrodynamic description. Since gravitational collapse can be studied numerically, holography provides a unique arena to study all stages of evolution — from far-from-equilibrium dynamics to hydrodynamics — in a microscopically complete and controlled setting. This has prompted much interest in using holographic theories as toy models of real quark-gluon plasma (for a review see [10]). The simplest theory with a dual holographic description is $\mathcal{N} = 4$ supersymmetric Yang-Mills theory (SYM), which is dual to gravity in AdS_5 .

A simple model of quark-gluon plasma production is the collision of gravitational shock waves [11–20], which can result in the formation of a black hole. The profile of the gravitational waves encodes the profile of colliding shock waves in the dual field theory. In this Letter we report on shock wave collisions in SYM, which superficially at least, resemble proton-nucleus collisions, with the “nucleus” represented as a planar shock wave and the “proton” represented by shock wave localized in the transverse directions. We use quotes here to emphasize

to the reader that the objects we are colliding are not bound states in QCD, but rather caricatures in SYM. The precollision geometry contains a trapped surface and the collision results in the formation of a black brane. We numerically solve the full 5D Einstein equations for the geometry after the collision and report on the evolution of the SYM stress tensor $T^{\mu\nu}$ and test the validity of hydrodynamics.

In strongly coupled SYM the hydrodynamic gradient expansion of $T^{\mu\nu}$ is an expansion in powers of $1/(\ell T_{\text{eff}})$ with ℓ the characteristic scale over which $T^{\mu\nu}$ varies and T_{eff} the effective temperature [21, 22]. Hence in strongly coupled SYM the microscopic scale $1/T_{\text{eff}}$ plays the role of the mean free path. We focus on the low energy limit, where T_{eff} is small and $1/T_{\text{eff}}$ is large, and demonstrate that collisions can result in the formation of droplets of liquid with sizes as small as $R \sim 1/T_{\text{eff}}$. Our results bolster the notion that debris produced in proton-nucleus collisions may be modeled using hydrodynamics.

Gravitational formulation.— We construct initial data for Einstein’s equations by superimposing the metric of gravitational shock waves moving in the $\pm z$ directions at the speed of light. In Fefferman-Graham coordinates the metric of a single shock moving in the $\pm z$ direction is

$$ds^2 = r^2 \left[-dt^2 + d\mathbf{x}^2 + \frac{dr^2}{r^4} + h_{\pm}(\mathbf{x}_{\perp}, z_{\mp}, r) dz_{\mp}^2 \right], \quad (1)$$

where $\mathbf{x} \equiv \{x, y, z\}$, $\mathbf{x}_{\perp} \equiv \{x, y\}$, $z_{\mp} \equiv z \mp t$, and

$$h_{\pm}(\mathbf{x}_{\perp}, z_{\mp}, r) \equiv \int \frac{d^2 k}{(2\pi)^2} e^{i\mathbf{k} \cdot \mathbf{x}_{\perp}} \tilde{H}_{\pm}(\mathbf{k}, z_{\mp}) \frac{8I_2(k/r)}{k^2 r^2}. \quad (2)$$

The boundary of the spacetime lies at $r = \infty$. The metric (1) is an exact solution to Einstein’s equations for any choice of \tilde{H}_{\pm} [11, 23]. This geometry represents a state in the dual SYM theory with stress-energy tensor [29]

$$T^{00} = T^{zz} = \pm T^{0z} = H_{\pm}(\mathbf{x}_{\perp}, z_{\mp}), \quad (3)$$

(and all other components vanishing), where H_{\pm} is the transverse Fourier transform of \tilde{H}_{\pm} . We choose the waves moving in the $+z$ and $-z$ directions to represent the “proton” and “nucleus” respectively.

A simple choice of shock profiles is

$$H_{\pm}(\mathbf{x}_{\perp}, z_{\mp}) = \mu_{\pm}(\mathbf{x}_{\perp})^3 \delta_w(z_{\mp}) \quad (4)$$

where $\delta_w(z_{\mp})$ is a smeared delta function with width w . On the boundary the longitudinally integrated energy density per unit area is $\mu_{\pm}(\mathbf{x}_{\perp})^3$. Note that under a boost in the z direction (and in the $w \rightarrow 0$ limit) only the normalization of μ_{\pm} change. We may therefore work in the frame in which $\max(\mu_+) = \max(\mu_-)$. For numerical convenience we chose $\mu_+(\mathbf{x}_{\perp})^3 = e^{-\frac{1}{2}\mathbf{x}_{\perp}^2/\sigma^2}$ with $\sigma = 3$, and $\mu_-(\mathbf{x}_{\perp})^3 = 1$. Hence, the “proton” stress is localized about $z = t$, $\mathbf{x}_{\perp} = 0$, and the “nucleus” stress is localized about $z = -t$ and is translationally invariant in the transverse plane. Our choice of energy scale $\mu_{\pm}(\mathbf{x}_{\perp}=0) = 1$ fixes units in the results presented below. For the smeared longitudinal δ function we use a Gaussian $\delta_w(z) = \frac{1}{\sqrt{2\pi w^2}} e^{-\frac{1}{2}z^2/w^2}$ with width $w = 0.375$. Note that evolution inside the future light cone of planar shock collisions with width $w = 0.375$ well approximates that of the δ function limit [24].

For early times, $t \ll -w$, the profiles H_{\pm} have negligible overlap and the precollision geometry can be constructed from (1) by replacing the last term with the sum of corresponding terms from left and right moving shocks. The resulting metric satisfies Einstein’s equations, at early times, up to exponentially small errors.

To evolve the precollision geometry forward in time we use the characteristic formulation of gravitational dynamics in asymptotically AdS spacetimes discussed in detail in [25]. Our metric ansatz reads

$$ds^2 = r^2 g_{\mu\nu}(x, r) dx^{\mu} dx^{\nu} + 2 dr dt, \quad (5)$$

with Greek indices denoting spacetime boundary coordinates, $x^{\mu} = (t, x, y, z)$. Near the boundary, $g_{\mu\nu} = \eta_{\mu\nu} + g_{\mu\nu}^{(4)}/r^4 + O(1/r^5)$. The subleading coefficients $g_{\mu\nu}^{(4)}$ determine the SYM stress tensor,

$$T^{\mu\nu} = g_{\mu\nu}^{(4)} + \frac{1}{4} \eta_{\mu\nu} g_{00}^{(4)}. \quad (6)$$

To generate initial data for our characteristic evolution, we numerically transform the precollision metric in Fefferman-Graham coordinates to the metric ansatz (5) [30]. We periodically compactify spatial directions with transverse size $L_x = L_y = 24$ and longitudinal length $L_z = 9$. We begin time evolution at $t = -1.5$ and evolve to $t = 2.5$. Time evolution is performed using a spectral grid of size $N_x = N_y = 39$, $N_z = 155$ and $N_r = 48$.

Results.— In Fig. 1 we plot the energy density T^{00} (top) and momentum density T^{0i} (bottom) in the plane $y = 0$ at several values of time. (Note that the plots are rotationally invariant about the z axis.) The color scaling in the lower plots denotes $|T^{0i}|$ and the flow lines indicate the direction of T^{0i} . At time $t = -1.125$ the system consists of a planar sheet of energy (the “nucleus”) localized

at $z = 1.125$ and a localized lump of energy (the “proton”) centered at $z = -1.125$, $x = 0$, with transverse width $\sigma = 3$. These two distributions of energy move towards each other at the speed of light and collide at $t = z = 0$. Far away from $x = 0$, where there is little overlap between the “proton” and the “nucleus,” the collision has little effect on the future evolution of the “nucleus.” Indeed, at $x = \pm 12$ the “nucleus” simply continues to propagate at the speed of light with little change in the profile of the energy or momentum densities. However, at $|x| \sim \sigma$ both the “proton” and “nucleus” are dramatically altered by the collision event; the collision results in the “proton” punching a hole of transverse size $\sim \sigma$ in the “nucleus.” The resulting produced debris lies inside the light cone and subsequently expands both in the transverse and longitudinal directions. As we argue below, it is in the region $|x| \sim \sigma$ — set by the transverse size of the “proton” — that the system begins to behave hydrodynamically after the collision.

At time and length scales \gg than the microscopic scale $1/T_{\text{eff}}$, nonhydrodynamic degrees of freedom must relax, the evolution of $T^{\mu\nu}$ must be governed by hydrodynamics, and the dual black hole geometry must be governed by fluid/gravity duality [21, 22]. The salient hydrodynamic variables are the fluid velocity u^{μ} and the proper energy ϵ , which near equilibrium are related to T_{eff} by

$$T_{\text{eff}} = \left(\frac{4\epsilon}{3\pi^4}\right)^{1/4}. \quad (7)$$

To obtain ϵ and u^{μ} , we extract the eigenvalues $p_{(\lambda)}$ and associated eigenvectors $e_{(\lambda)}^{\mu}$ of $T^{\mu\nu}$,

$$T^{\mu}_{\nu} e_{(\lambda)}^{\nu} = p_{(\lambda)} e_{(\lambda)}^{\mu}, \quad (8)$$

with no sum over λ implied. Near equilibrium T^{μ}_{ν} has one timelike eigenvector, $e_{(0)}^{\mu}$, and three spacelike eigenvectors, $e_{(i)}^{\mu}$. The temporal eigenvalue is simply the proper energy, $\epsilon \equiv -p_{(0)}$, with the local fluid velocity the associated eigenvector, $u^{\mu} \equiv e_{(0)}^{\mu}$. We choose normalization $u_{\mu} u^{\mu} = -1$ with $u^0 > 0$. The spatial eigenvalues $p_{(i)}$ represent local pressures in the fluid rest frame. With the complete spacetime dependence of the flow field u^{μ} and energy density ϵ determined from the exact stress, we then construct the hydrodynamic approximation to the stress tensor $T_{\text{hydro}}^{\mu\nu}$ using the constitutive relations of 2nd order conformal hydrodynamics with transport coefficients determined by fluid/gravity duality [21, 22].

In Fig. 2 we plot the stress tensor components T^{xx} and T^{zz} , and their hydrodynamic approximations at $\mathbf{x} = 0$ as a function of time. At this point $\mathbf{u} = O(10^{-2})$, the stress tensor is approximately diagonal, and the local fluid pressures are well approximated by T^{xx} and T^{zz} . The pressures increase dramatically during the collision, reflecting a system which is highly anisotropic and far from equilibrium. However, after time $t = t_{\text{hydro}} \sim 1.2$ there is a qualitative change in the behavior of T^{xx} and

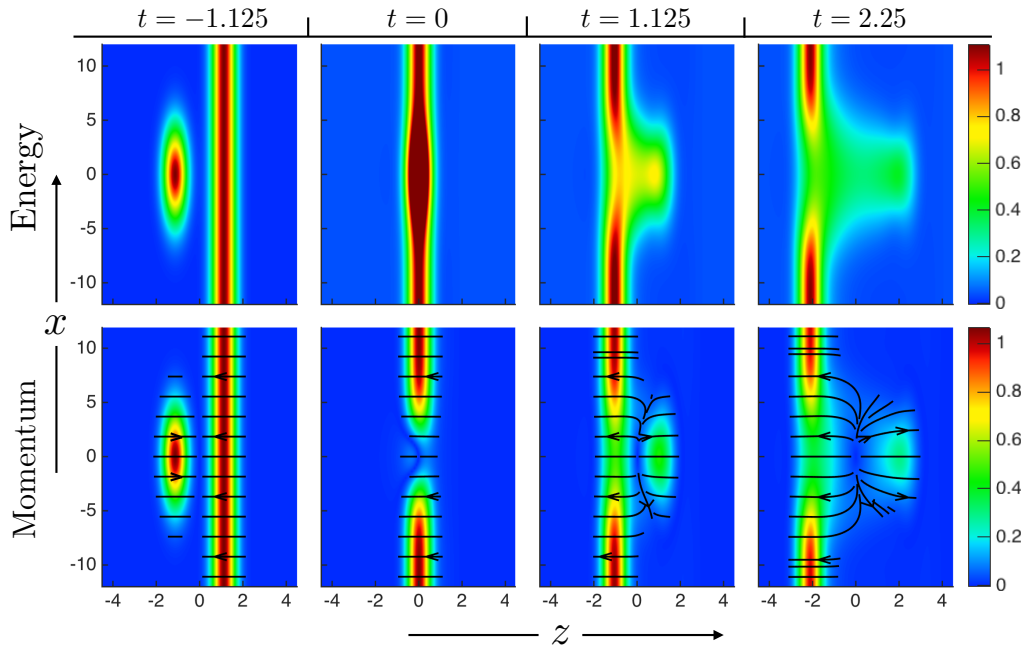


FIG. 1: The energy density T^{00} (top) and momentum density $|T^{0i}|$ (bottom), at four different times, in the plane $y = 0$. Streamlines in the lower plots denote the direction of T^{0i} . The stress is rotationally invariant about the z axis. At time $t = -1.125$ the “nucleus” is at $z = 1.125$ and the “proton” is at $z = -1.125$. These two distributions of energy move towards each other at the speed of light and collide at $t = z = 0$. Note that the color scaling for the energy at $t = 0$ is off scale. Far away from $x = 0$, where there is little overlap between the “proton” and the “nucleus,” the collision has little effect on the future evolution of the “nucleus.” However, near $x = 0$ the “proton” punches a hole in the “nucleus.” The resulting debris has transverse size of order that of the “proton,” lies inside the light cone and expands in the transverse and longitudinal directions.

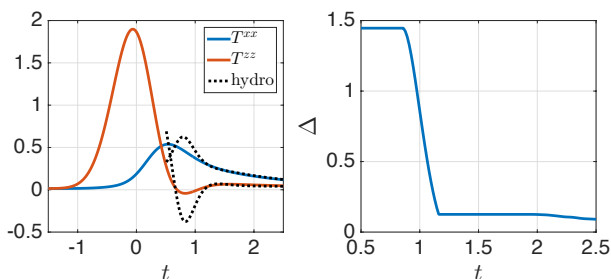


FIG. 2: Left: Stress tensor components T^{xx} and T^{zz} at $\mathbf{x} = 0$ as a function of time together with their hydrodynamic approximation. Around $t = 0$ the system is highly anisotropic and far from equilibrium. Nevertheless, at this point in space, the system begins to evolve hydrodynamically at $t \approx 1.2$. Right: the hydrodynamic residual Δ at $\mathbf{x} = 0$ as a function of time. After $t = 1.2$, $\Delta < 0.13$.

T^{zz} ; thereafter the stress slowly varies in time and slowly isotropizes. Likewise, after t_{hydro} the pressures are well described by the hydrodynamic constitutive relations.

To elaborate on the domain of utility of hydrodynamics we define the dimensionless residual measure

$$\Delta(t, \mathbf{x}) \equiv \max_{t' \geq t} \left(\frac{1}{\bar{p}(t', \mathbf{x})} \sqrt{\Delta T_{\mu\nu}(t', \mathbf{x}) \Delta T^{\mu\nu}(t', \mathbf{x})} \right), \quad (9)$$

with $\Delta T^{\mu\nu} \equiv T^{\mu\nu} - T_{\text{hydro}}^{\mu\nu}$ and $\bar{p} \equiv \frac{1}{3} \sum_i p(i) = \frac{\epsilon}{3}$ the average pressure. In the local fluid rest frame $\Delta T^{\mu\nu} \Delta T_{\mu\nu} = \Delta T^{ij} \Delta T_{ij}$. Note that $\Delta T^{\mu\nu} \Delta T_{\mu\nu}$ is in general nonmonotonic in time due to nonhydrodynamic modes, such as quasinormal modes, oscillating in time while decaying. Indeed, T^{xx} and T^{zz} in Fig. 2 agree with the hydrodynamic constitutive relations at $t \approx 0.65$, but subsequently disagree until $t \gtrsim 1.2$. Taking the max in (9) ameliorates the effect of the oscillations and aids in avoiding the false identification of hydrodynamic evolution if $\Delta T^{\mu\nu} \Delta T_{\mu\nu}$ is temporarily small. If $\Delta \ll 1$ at t, \mathbf{x} , then $T^{\mu\nu}$ is well described by the hydrodynamic constitutive relations at \mathbf{x} at time t and all later times. Also included in Fig. 2 is a plot of Δ at $\mathbf{x} = 0$ as a function of time. During the collision $\Delta \sim 1$ and $T^{\mu\nu}$ is not described by hydrodynamics. However, after $t \sim 0.8$, Δ rapidly decays and after $t = 1.2$, $\Delta < 0.13$. In what follows we use $\Delta \lesssim 0.2$ as a litmus test for whether the evolution of $T^{\mu\nu}$ is consistent with the hydrodynamic constitutive relations.

In the remaining plots Figs. 3(a)-3(f) we restrict our attention to time $t = 1.5$ and to the region in the $x-z$ plane in where $\Delta \leq 0.2$. We explain the coloring of the different plots below. The stress in the omitted regions has $\Delta > 0.2$ and is not well approximated by the hydrodynamic constitutive relations. All plots in Fig. 3 include

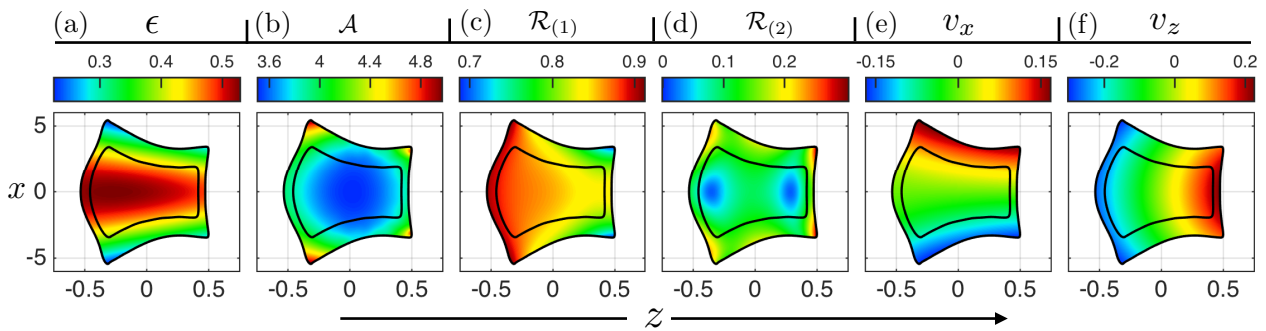


FIG. 3: From left to right: the proper energy ϵ , the anisotropy \mathcal{A} , the first and second order gradient measures $\mathcal{R}_{(1)}$ and $\mathcal{R}_{(2)}$, and the transverse and longitudinal fluid velocities v_x and v_z respectively. All plots are shown at time $t = 1.5$ and are restricted to the domain $\Delta \leq 0.2$ and are rotationally invariant about the z axis. The outer (inner) contours in all plots are $\Delta = 0.2$ (0.15), with $\Delta < 0.2$ (0.15) everywhere inside. In the displayed region, which has transverse radius $R \sim 1/T_{\text{eff}}$, hydrodynamics is a good description of the evolution of the stress.

the same $\Delta = \text{const.}$ contours. The outer (inner) contour is $\Delta = 0.2$ (0.15), with $\Delta < 0.2$ (0.15) everywhere inside. The transverse radius of these contours is $R \sim 4$, which is approximately that of the initial “proton” seen in Fig. 1. We therefore conclude that the collision results in the formation of a droplet of liquid with transverse size of order that of the “proton.” The color scaling in Fig. 3(a) denotes the proper energy ϵ . In the plotted domain the average ϵ is ~ 0.4 and, via (7), the average T_{eff} is ~ 0.25 . We therefore obtain the dimensionless measure of the transverse size of the drop of liquid,

$$RT_{\text{eff}} \sim 1. \quad (10)$$

Evidently, hydrodynamics works even when the system size is of order the microscopic scale $1/T_{\text{eff}}$. Additionally, note $t_{\text{hydro}}T_{\text{eff}} \sim 0.3$. Similar hydrodynamization times were observed in the 1+1 dimensional flows of [14, 16, 26] with $t_{\text{hydro}}T_{\text{eff}} \sim 0.3$ appearing as a lower bound.

When $R \sim 1/T_{\text{eff}}$ it is natural to expect gradients to be large. In order to quantify the size of gradients we define the anisotropy function

$$\mathcal{A} \equiv \max(p_{(i)})/\min(p_{(i)}). \quad (11)$$

In ideal hydrodynamics, where the stress is isotropic in the local rest frame, $\mathcal{A} = 1$. Therefore, deviations of \mathcal{A} from 1 in regions where $\Delta \ll 1$ must be due to gradient corrections to the hydrodynamic constitutive relations. In Fig. 3(b) we plot \mathcal{A} . In the displayed domain $\mathcal{A} \sim 4$. Evidently, gradients are large and ideal hydrodynamics is not a good approximation.

However, the observed anisotropy is almost entirely due to first order viscous effects alone. To see this, let $\Pi_{(n)}^{\mu\nu}$ be the n^{th} order contribution to the viscous stress and define the dimensionless gradient measures

$$\mathcal{R}_{(n)} \equiv \frac{1}{p} \sqrt{\Pi_{(n)\mu\nu}\Pi_{(n)}^{\mu\nu}}. \quad (12)$$

In the local rest frame $\Pi_{(n)\mu\nu}\Pi_{(n)}^{\mu\nu} = \Pi_{(n)ij}\Pi_{(n)}^{ij}$. $\mathcal{R}_{(n)}$ measures the size of the n^{th} order gradients corrections relative to ideal hydrodynamics. In Figs. 3(c)-3(d) we plot $\mathcal{R}_{(1)}$ and $\mathcal{R}_{(2)}$. Inside the $\Delta = 0.15$ contour $\mathcal{R}_{(1)} \sim 0.85$ and $\mathcal{R}_{(2)} \sim 0.1$. Hence, first order gradient corrections are as large as the ideal stress with the second order correction an order of magnitude smaller. Similar observations were made in [14, 26] within the context boost invariant flow.

Discussion.—Given that $1/T_{\text{eff}}$ is the salient microscopic scale in strongly coupled plasma — akin to a mean free path at weak coupling — it is remarkable that hydrodynamics can describe the evolution systems as small as $R \sim 1/T_{\text{eff}}$. Simply put, even when $R \sim 1/T_{\text{eff}}$ and gradients are large, nonhydrodynamic modes decay and the hydrodynamic gradient expansion is well behaved.

It should be noted that upon fixing units by setting σ equal to the proton radius, $\sigma \sim 1$ fm, in the c.m. frame our “proton” has energy ~ 20 GeV and the effective temperature of the produced plasma is $T_{\text{eff}} \sim 200$ MeV. Given that proton-nucleus collisions at RHIC and the LHC have energies and temperatures greater than this, it is natural to expect RT_{eff} to be larger in RHIC and LHC collisions than the simulated collision presented here. Given that hydrodynamics already works well when $RT_{\text{eff}} \sim 1$, our observed extreme applicability of hydrodynamics, both in terms of the system size and the size of gradients, bolsters the notion the debris produced in proton-nucleus collisions can be modeled with hydrodynamics.

However, hydrodynamic simulations of tiny short lived systems with large gradients will likely be sensitive to the initial viscous stress, which Figs. 3(b)-3(c) demonstrate is large, and to the initial transverse fluid velocity. Indeed, as shown in Fig. 3(e)-3(f), the transverse and longitudinal components of the fluid 3-velocity $\mathbf{v} \equiv \mathbf{u}/u^0$ are similar in magnitude. Simply put, large gradients result in large viscous stress and drive the rapid development

of transverse flow. These effects are likely key ingredients in initial hydrodynamic data required for precision modeling of proton-nucleus collisions.

It would be interesting to push our analysis further: how big are the smallest drops of liquid? Clearly RT_{eff} cannot be made arbitrarily small since the hydrodynamic gradient expansion is badly behaved when $RT_{\text{eff}} \ll 1$. Additionally, in the gravitational description there should exist a critical energy E_c , below which no black hole is formed, and which for $E = E_c + 0^+$ critical gravitational collapse occurs [27]. The absence of a black hole when $E < E_c$ means that in the dual field theory the collisional debris will not evolve hydrodynamically at any future time. It would be interesting to study dynamics near E_c and the signatures of hydrodynamics turning off.

Acknowledgments.—I am grateful to Janet Johnson, Krishna Rajagopal and Subir Sachdev for assistance with computer resources required to complete this project. This work is supported by the Fundamental Laws Initiative of the Center for the Fundamental Laws of Nature at Harvard University.

* Electronic address: pchesler@physics.harvard.edu

- [1] **CMS** Collaboration, S. Chatrchyan *et al.*, “Multiplicity and transverse momentum dependence of two- and four-particle correlations in pPb and PbPb collisions,” *Phys.Lett.* **B724** (2013) 213–240, [arXiv:1305.0609 \[nucl-ex\]](#).
- [2] **ALICE** Collaboration, B. Abelev *et al.*, “Long-range angular correlations on the near and away side in p -Pb collisions at $\sqrt{s_{NN}} = 5.02$ TeV,” *Phys.Lett.* **B719** (2013) 29–41, [arXiv:1212.2001 \[nucl-ex\]](#).
- [3] **ATLAS** Collaboration, G. Aad *et al.*, “Observation of Associated Near-Side and Away-Side Long-Range Correlations in $\sqrt{s_{NN}}=5.02$ TeV Proton-Lead Collisions with the ATLAS Detector,” *Phys.Rev.Lett.* **110** (2013) no. 18, 182302, [arXiv:1212.5198 \[hep-ex\]](#).
- [4] **PHENIX** Collaboration, A. Adare *et al.*, “Quadrupole Anisotropy in Dihadron Azimuthal Correlations in Central d +Au Collisions at $\sqrt{s_{NN}}=200$ GeV,” *Phys.Rev.Lett.* **111** (2013) no. 21, 212301, [arXiv:1303.1794 \[nucl-ex\]](#).
- [5] A. Dumitru, L. McLerran, and V. Skokov, “Azimuthal asymmetries and the emergence of collectivity from multi-particle correlations in high-energy pA collisions,” *Phys.Lett.* **B743** (2015) 134–137, [arXiv:1410.4844 \[hep-ph\]](#).
- [6] P. Bozek, “Collective flow in p-Pb and d-Pd collisions at TeV energies,” *Phys.Rev.* **C85** (2012) 014911, [arXiv:1112.0915 \[hep-ph\]](#).
- [7] P. Bozek and W. Broniowski, “Correlations from hydrodynamic flow in p-Pb collisions,” *Phys.Lett.* **B718** (2013) 1557–1561, [arXiv:1211.0845 \[nucl-th\]](#).
- [8] A. Bzdak, B. Schenke, P. Tribedy, and R. Venugopalan, “Initial state geometry and the role of hydrodynamics in proton-proton, proton-nucleus and deuteron-nucleus collisions,” *Phys.Rev.* **C87** (2013) no. 6, 064906, [arXiv:1304.3403 \[nucl-th\]](#).
- [9] J. M. Maldacena, “The large N limit of superconformal field theories and supergravity,” *Adv. Theor. Math. Phys.* **2** (1998) 231–252, [hep-th/9711200](#).
- [10] J. Casalderrey-Solana, H. Liu, D. Mateos, K. Rajagopal, and U. A. Wiedemann, “Gauge/String Duality, Hot QCD and Heavy Ion Collisions,” [arXiv:1101.0618 \[hep-th\]](#).
- [11] D. Grumiller and P. Romatschke, “On the collision of two shock waves in AdS₅,” *JHEP* **08** (2008) 027, [arXiv:0803.3226 \[hep-th\]](#).
- [12] J. L. Albacete, Y. V. Kovchegov, and A. Taliotis, “Modeling heavy ion collisions in AdS/CFT,” *JHEP* **0807** (2008) 100, [arXiv:0805.2927 \[hep-th\]](#).
- [13] J. L. Albacete, Y. V. Kovchegov, and A. Taliotis, “Asymmetric collision of two shock waves in AdS₅,” *JHEP* **0905** (2009) 060, [arXiv:0902.3046 \[hep-th\]](#).
- [14] P. M. Chesler and L. G. Yaffe, “Boost invariant flow, black hole formation, and far-from-equilibrium dynamics in $\mathcal{N} = 4$ supersymmetric Yang-Mills theory,” *Phys.Rev.* **D82** (2010) 026006, [arXiv:0906.4426 \[hep-th\]](#).
- [15] P. M. Chesler and L. G. Yaffe, “Holography and colliding gravitational shock waves in asymptotically AdS₅ spacetime,” *Phys.Rev.Lett.* **106** (2011) 021601, [arXiv:1011.3562 \[hep-th\]](#).
- [16] J. Casalderrey-Solana, M. P. Heller, D. Mateos, and W. van der Schee, “From full stopping to transparency in a holographic model of heavy ion collisions,” *Phys.Rev.Lett.* **111** (2013) 181601, [arXiv:1305.4919 \[hep-th\]](#).
- [17] W. van der Schee, P. Romatschke, and S. Pratt, “Fully dynamical simulation of central nuclear collisions,” *Phys.Rev.Lett.* **111** (2013) no. 22, 222302, [arXiv:1307.2539](#).
- [18] H. Bantilan, F. Pretorius, and S. S. Gubser, “Simulation of asymptotically AdS₅ spacetimes with a generalized harmonic evolution scheme,” *Phys.Rev.* **D85** (2012) 084038, [arXiv:1201.2132 \[hep-th\]](#).
- [19] H. Bantilan and P. Romatschke, “Simulation of black hole collisions in asymptotically AdS spacetimes,” [arXiv:1410.4799 \[hep-th\]](#).
- [20] P. M. Chesler and L. G. Yaffe, “Holography and off-center collisions of localized shock waves,” [arXiv:1501.04644 \[hep-th\]](#).
- [21] S. Bhattacharyya, V. E. Hubeny, S. Minwalla, and M. Rangamani, “Nonlinear fluid dynamics from gravity,” *JHEP* **02** (2008) 045, [arXiv:0712.2456](#).
- [22] R. Baier, P. Romatschke, D. T. Son, A. O. Starinets, and M. A. Stephanov, “Relativistic viscous hydrodynamics, conformal invariance, and holography,” *JHEP* **04** (2008) 100, [arXiv:0712.2451](#).
- [23] S. S. Gubser, S. S. Pufu, and A. Yarom, “Entropy production in collisions of gravitational shock waves and of heavy ions,” *Phys. Rev.* **D78** (2008) 066014, [arXiv:0805.1551 \[hep-th\]](#).
- [24] P. M. Chesler, N. Kilbertus, and W. van der Schee, “Universal hydrodynamic flow in holographic planar shock collisions,” [arXiv:1507.02548 \[hep-th\]](#).
- [25] P. M. Chesler and L. G. Yaffe, “Numerical solution of gravitational dynamics in asymptotically anti-de Sitter spacetimes,” *JHEP* **1407** (2014) 086, [arXiv:1309.1439 \[hep-th\]](#).
- [26] M. P. Heller, R. A. Janik, and P. Witaszczyk,

- “Hydrodynamic Gradient Expansion in Gauge Theory Plasmas,” *Phys.Rev.Lett.* **110** (2013) no. 21, 211602, [arXiv:1302.0697 \[hep-th\]](#).
- [27] M. W. Choptuik, “Universality and scaling in gravitational collapse of a massless scalar field,” *Phys.Rev.Lett.* **70** (1993) 9–12.
- [28] S. de Haro, S. N. Solodukhin, and K. Skenderis, “Holographic reconstruction of space-time and renormalization in the AdS / CFT correspondence,” *Commun.Math.Phys.* **217** (2001) 595–622, [arXiv:hep-th/0002230 \[hep-th\]](#).
- [29] In Eq. (3), and thereafter, $T^{\mu\nu}$ is really the expectation value of the SYM stress-energy tensor divided by $N_c^2/(2\pi^2)$, with N_c the gauge group rank [28]. In computing the “proton” energy below, we use $N_c = 3$.
- [30] We also modify the initial data by adding a small uniform background energy density, equal to 4% of the peak energy density of the incoming shocks. This allows use of a coarser grid, reducing memory requirements.